



## Thiazole-based chemosensor: synthesis and ratiometric fluorescence sensing of zinc

Aasif Helal, Hong-Seok Kim \*

Department of Applied Chemistry, Kyungpook National University, Daegu 702-701, Republic of Korea

### ARTICLE INFO

#### Article history:

Received 31 May 2009

Revised 14 July 2009

Accepted 16 July 2009

Available online 18 July 2009

#### Keywords:

Thiazole

Ratiometric sensing of Zn<sup>2+</sup>

ESIPT

Fluorescence

### ABSTRACT

A new ratiometric and selective fluorescent chemosensor (**1**), based on thiazole for quantification of zinc ions in aqueous ethanol, was synthesized and investigated. The mechanism of fluorescence was based on the cation-induced inhibition of excited-state intramolecular proton transfer (ESIPT).

© 2009 Elsevier Ltd. All rights reserved.

A fluorescent chemosensor consists of a molecular system for which the physicochemical properties change upon interaction with a chemical species, in such a way as to produce a detectable fluorescent signal.<sup>1</sup> Zinc(II) is the second most abundant transition-metal form of cation in the biological system.<sup>2</sup> Approximately 300 enzymes contain zinc(II) as an essential component, either for a structural purpose or as a part of a catalytic site. For example, zinc is essential for the regulation of DNA synthesis during the proliferation and differentiation of cells.<sup>3</sup> Zinc is also known to have a role in neurological disorders, such as Parkinson's disease, Alzheimer's disease, amyotrophic lateral sclerosis, and epileptic seizures.<sup>4</sup> Therefore, the design and development of a fluorescent chemosensor selective to zinc are of considerable interest.

A variety of zinc ion selective fluorescent probes that are based on quinoline,<sup>5</sup> fluorescein,<sup>6</sup> coumarin,<sup>7</sup> indole,<sup>8</sup> and other fluorophores<sup>9</sup> or proteins<sup>10</sup> have been developed. But a majority of these zinc sensors function as cation-responsive optical switches that translate the binding event into either an increase or decrease of the emission intensity.<sup>11</sup> However, the emission intensity is also dependent on other factors, such as the sensor concentration, bleaching, optical path length, and illumination intensity. It is therefore desirable to eliminate the effects of these factors by using a ratiometric sensor that exhibits a spectral shift upon reaction or binding to the analyte of interest. The ratio between the two emission intensities can be used to evaluate the analyte concentration.<sup>12</sup> Excited-state intramolecular proton transfer (ESIPT) is one

of the most common photophysical processes that occurs in benzazoles and used to develop ratiometric probes. Inhibition of the ESIPT process by cation binding yields a significant hypsochromic shift of the fluorescence emission maximum.<sup>13,14</sup>

Crown ethers that contain thiazole moieties<sup>15</sup> have been reported to exhibit large ammonium ion selectivity.<sup>14b</sup> Benzene-based tripodal receptors<sup>16,17</sup> and steroidal tweezers<sup>18,19</sup> have been used for selective detection of silver(I) by introduction of soft heteroatoms N and S, as electron donors to metal cations. However application of heteroaromatic ring system such as thiazole, which contains soft heteroatoms N and S and has substitutes at positions 2 and 4 as a zinc chemosensor has not yet been reported.

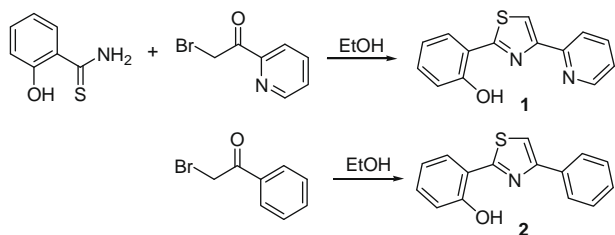
In this Letter, design and development of a novel thiazole-based ratiometric fluorescent chemosensor with substitutes at positions 2 and 4 regarding zinc ion in aqueous media are reported. It exhibits a ratiometric fluorescent response upon addition of zinc ion into 10% water in ethanol, buffered at pH 7.4. The results obtained from investigation on effect of solvents and competitive processes of zinc cation with other cations are reported.

ESIPT is one of the most common photophysical properties that occurs in benzazoles used to develop ratiometric probes. In order to understand the crucial role of both phenol and pyridine rings providing a suitable binding site for zinc ion, **1** and **2** were prepared in good yields by the reaction of 2-hydroxythiobenzamide with 2-(2-bromoacetyl)pyridine and 2-bromoacetophenone in refluxing ethanol, as shown in Scheme 1. The structures of **1** and **2** were confirmed by <sup>1</sup>H NMR, <sup>13</sup>C NMR, and elemental analyses data.

Initial studies on the UV–vis absorption and fluorescent emission processes revealed that **1** showed selectivity toward zinc

\* Corresponding author. Tel.: +82 53 950 5588; fax: +82 53 950 6594.

E-mail address: [kimhs@knu.ac.kr](mailto:kimhs@knu.ac.kr) (H.-S. Kim).



**Scheme 1.** Synthesis of 4-pyridylthiazole (**1**) and 4-phenylthiazole (**2**).

cation in  $\text{CH}_3\text{CN}$ . As shown in Figure 1, in the absence of zinc **1** showed an absorption band at 331 nm and a fluorescent emission

at 481 nm, whereas in the presence of zinc **1** revealed absorption and emission bands at 390 and 461 nm, respectively. Coordination of zinc cation to **1** causes a red shift in UV-vis absorption and a blue shift in fluorescent spectrum along with enhancement in the degree of intensity.

In contrast to 4-pyridylthiazole (**1**), 4-phenylthiazole (**2**) which has no pyridine moiety has not revealed any significant changes in absorption and fluorescence emissions upon addition of up to 10 equiv of zinc ion as shown in Figure 1.

Compound **1**, bearing the 2-hydroxyphenyl-thiazole signaling unit and pyridine as the binding site, is anticipated to act as an ESIPT-based chemosensor. The changes of absorption spectra of **1** upon addition of zinc perchlorate showed three different stages

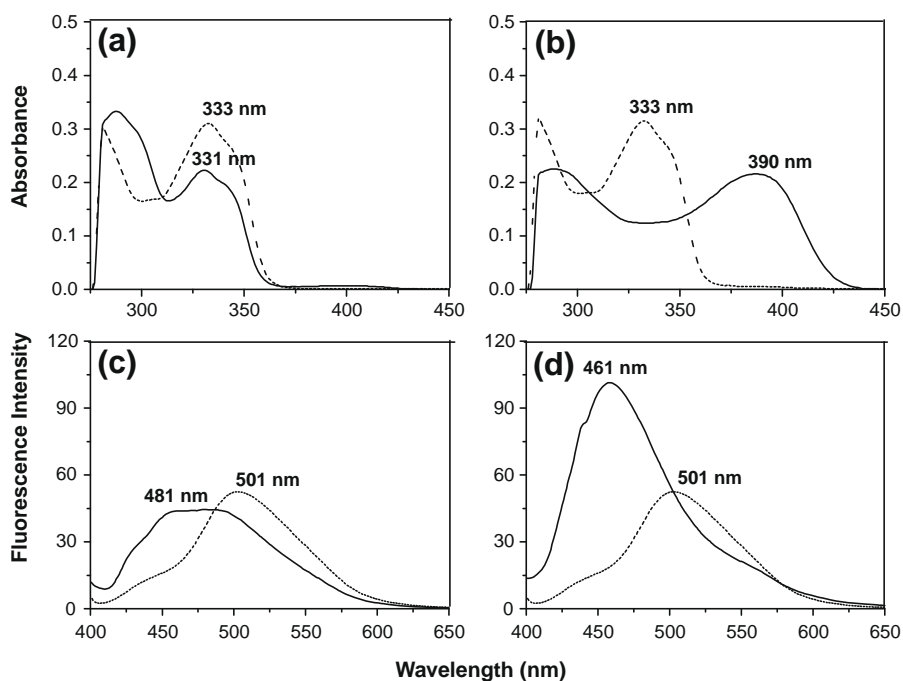


**Figure 1.** UV-vis spectra of **1** (—) and **2** (---) (a) in the absence, and (b) in the presence of 10 equiv of  $\text{Zn}(\text{ClO}_4)_2$  in dry  $\text{CH}_3\text{CN}$ . Fluorescence spectra of **1** (—) and **2** (---) (c) in the absence and (d) in the presence of 10 equiv of  $\text{Zn}(\text{ClO}_4)_2$  in dry  $\text{CH}_3\text{CN}$ .

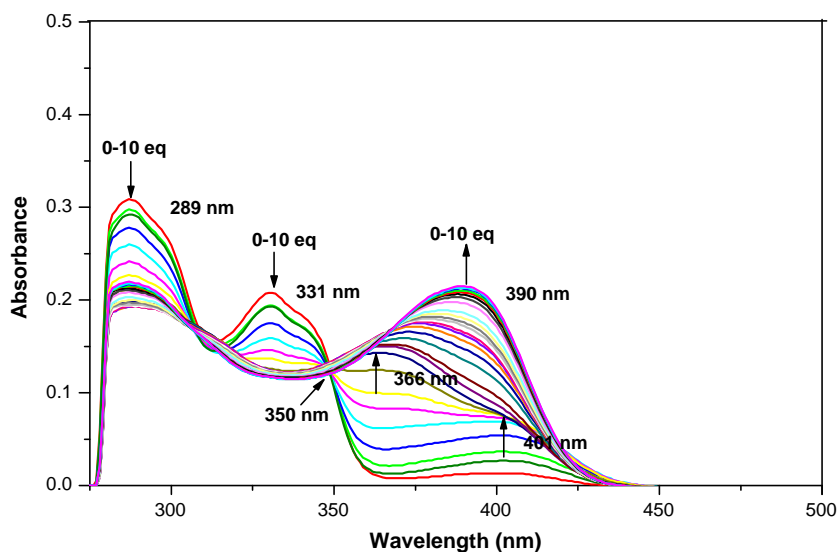


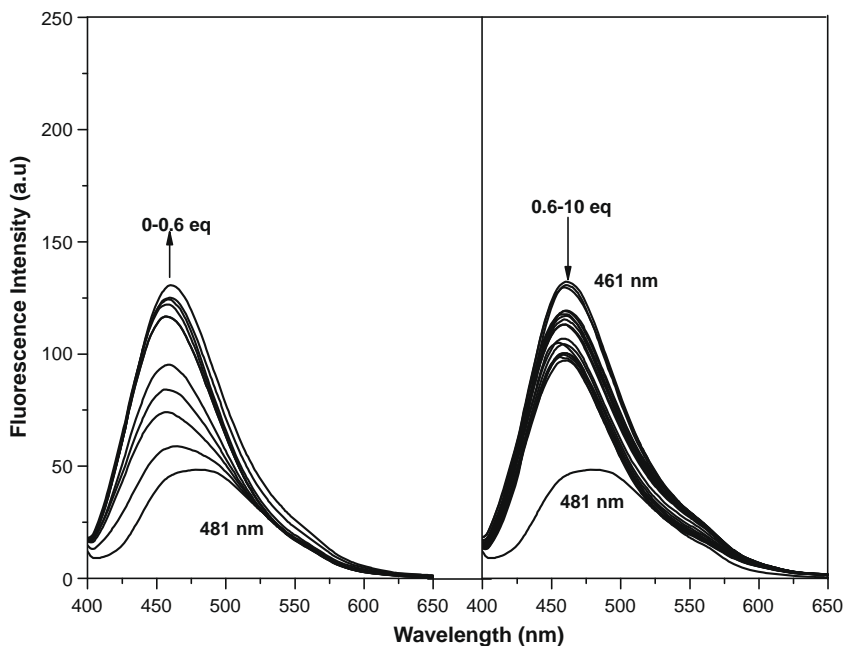
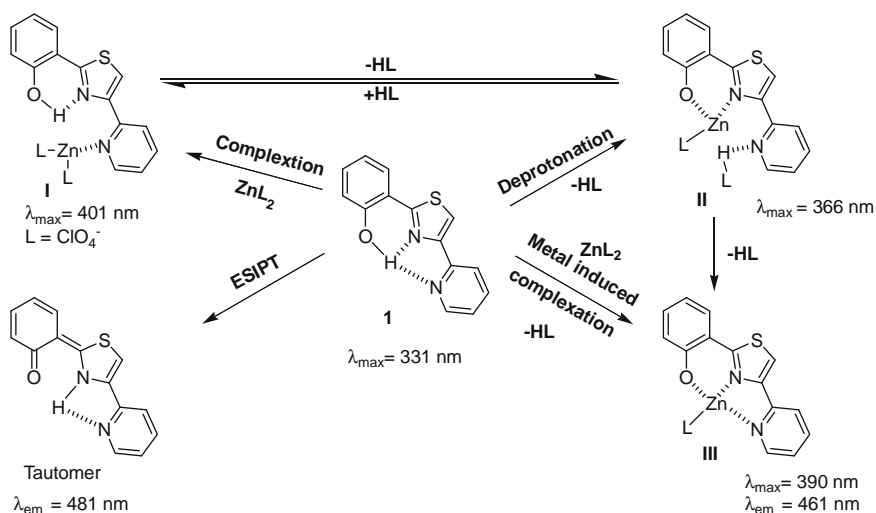
**Figure 2.** Changes in UV-vis spectra of **1** (20  $\mu\text{M}$ ) upon addition of  $\text{Zn}(\text{ClO}_4)_2$  in dry  $\text{CH}_3\text{CN}$ .

as shown in Figure 2. At the initial stage of addition (0–0.3 equiv) peak develops at 401 nm which is due to the binding of zinc with the nitrogen of pyridine (Form I). Upon the further addition of zinc (0.3–0.6 equiv) this peak gradually disappears and a new peak at 366 nm appears in the second stage which is attributed to the concomitant deprotonation of the phenolic proton and protonation of the pyridine nitrogen (Form II). In the final step (0.6–1 equiv) zinc coordinates with the nitrogen of the pyridine ring to give peak at 390 nm (Form III). Thus the absorption band at 390 nm becomes saturated up to 1 equiv of zinc. These possible forms of **1** with different amounts of zinc in ground and excited states are depicted in Scheme 2.

The fluorescence titration spectra of **1** with zinc cation show an emission maximum peak at 481 nm (Fig. 3). Upon addition of zinc up to 0.6 equiv emission band at 481 nm undergoes a hypsochromic shift and enhancement to 461 nm gradually. This is attributed to the inhibition of ESIPT by deprotonation of the phe-

nolic proton. On further addition of zinc (0.6–1.0 equiv) this peak undergoes quenching due to binding with the nitrogen of the pyridine and saturates within the addition of 1 equiv of zinc. From the fluorescence titration, the binding constant for zinc ion is observed to be  $5.0 \times 10^5 \text{ M}^{-1}$  (Error estimated to be  $\leq 10\%$ ).

In order to achieve a more physiologically acceptable condition the photophysical properties of **1** were examined in an ethanol–water system. UV–vis study was carried out in 10% (v/v) water/ethanol buffered by 10 mM HEPES at pH 7.4 at a concentration level of 20  $\mu\text{M}$ . Sensor **1** displayed an obvious absorption band at 329 nm. This can be attributed to a  $\pi\text{-}\pi^*$  transition; this is favored by the planar orientation enforced by the intramolecular hydrogen bonding.<sup>20</sup> However, upon addition of zinc ion to the solution of **1**, the absorption band at 384 nm becomes enhanced gradually while the absorption band at 329 nm decreased synchronously, as shown in Figure 4. The absorption bands at 329 and 384 nm linearly



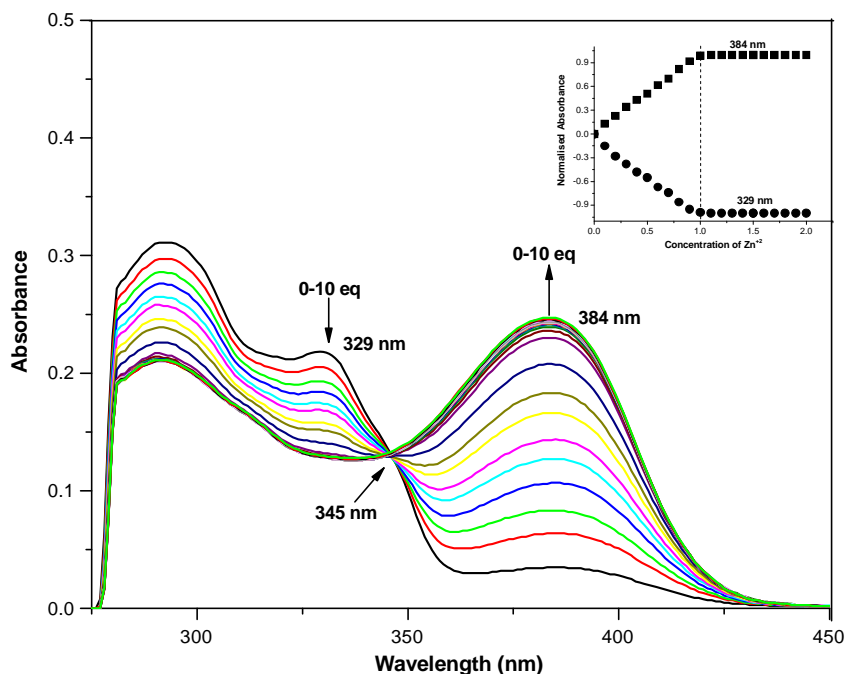


**Figure 4.** Changes in UV-vis spectra of **1** (20  $\mu\text{M}$ ) upon addition of  $\text{Zn}(\text{ClO}_4)_2$  in EtOH/ $\text{H}_2\text{O}$  (9:1) containing HEPES buffer (10 mM, pH 7.4). Inset: mol ratio plots of absorbance at 329 and 384 nm.

decreased and increased, respectively, up to 1 equiv of zinc (Fig. 4 inset), indicating the formation of a 1:1 complex with a strong binding affinity.

The Job's plot of **1** with zinc also indicates the formation of a 1:1 complex (Fig. S-1). The binding constant calculated in an ethanol-water system at pH 7.4 was  $3.5 \times 10^4 \text{ M}^{-1}$  (Error estimated to be  $\leq 10\%$ ).

Similarly, fluorescence titration of **1** with zinc was carried out in 10% (v/v) water/ethanol buffered by 10 mM HEPES at pH 7.4 at a

concentration level of 20  $\mu\text{M}$ . Addition of zinc ion to the solution of **1** causes a simultaneous blue shift of fluorescent emission from 502 to 461 nm when excited at 345 nm, with an isoemission point at 485 nm (Fig. 5). Like the benzothiazole derivatives<sup>13</sup> compounds **1** and **2** contain an intramolecular hydrogen bond that undergoes ESIPT and yields a highly Stokes'-shifted emission from the proton-transfer tautomer.<sup>21–23</sup> Coordination of zinc removes the phenolic proton and disrupts the ESIPT, thus causing emission with a normal Stokes' shift. The binding mode of **1** with zinc from the

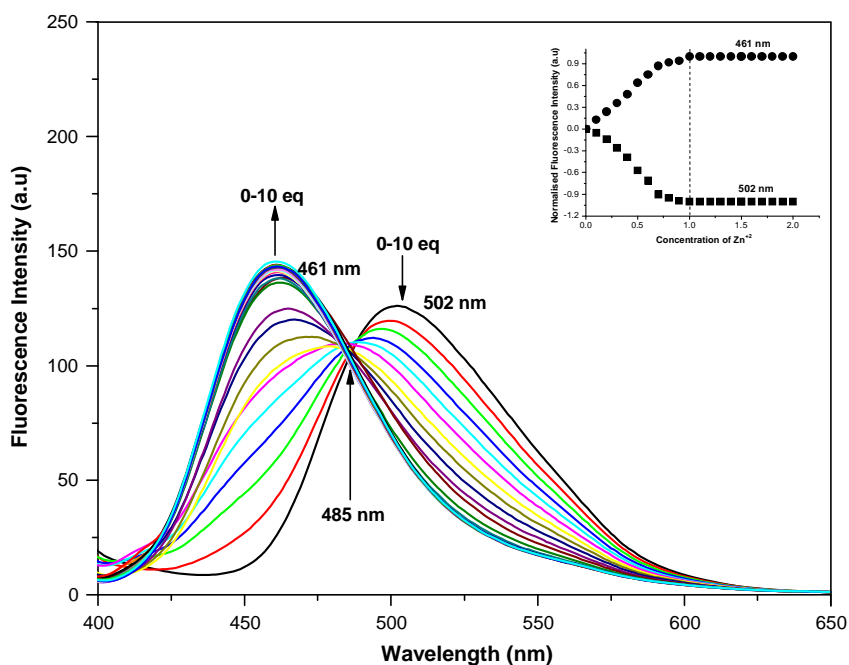


**Figure 5.** Changes in fluorescence spectra of **1** (20  $\mu\text{M}$ ) in EtOH/ $\text{H}_2\text{O}$  (9:1) containing HEPES buffer (10 mM, pH 7.4) upon addition of  $\text{Zn}(\text{ClO}_4)_2$ . ( $\lambda_{\text{ex}} = 345 \text{ nm}$ ) Inset: mol ratio plots of emission at 461 and 502 nm.

results of fluorescence titration spectra (Fig. 5 inset) and Job's plot (Fig. S-2) showed to be 1:1 with a binding constant  $3.2 \times 10^4 \text{ M}^{-1}$ . This value is smaller than that of the one obtained in an aprotic solvent  $\text{CH}_3\text{CN}$ . The photophysical properties of **1** and **2** are summarized in Table 1.

The selectivity and tolerance of **1** for zinc ion over other biologically relevant metal cations such as  $\text{Na}^+$ ,  $\text{K}^+$ ,  $\text{Mg}^{2+}$ ,  $\text{Ca}^{2+}$ , and non-biologically relevant metal cations were investigated by adding 10 equiv of metal cations to 20  $\mu\text{M}$  solution of **1**. There was no obvious blue shift to 461 nm in any other metal ions except zinc. The paramagnetic transition-metal cations  $\text{Co}^{2+}$ ,  $\text{Fe}^{2+}$ ,  $\text{Ni}^{2+}$ , and  $\text{Cu}^{2+}$  coordinate to **1**, but partially or completely quench the fluorescence emission (Fig. 6). The quenching results obtained with addition of these cations suggest that  $\text{Co}^{2+}$ ,  $\text{Fe}^{2+}$ ,  $\text{Ni}^{2+}$ , and  $\text{Cu}^{2+}$  which occupy open shell d-orbitals provide a very fast and efficient non-radiative decay of the excited states due to the electron or energy transfer between the metal cations and **1**. While  $\text{Zn}^{2+}$  cation, which has close shell d-orbitals, does not introduce low-energy metal-centered or charge-separated excited states energy and electron transfer processes cannot take place.<sup>24</sup> Fluorescence intensity ratio curve also suggests that only zinc undergoes a blue shift on coordination with **1** (Fig. 7). Competition binding experiment carried out with different metal ions (1.0 equiv) and zinc (Fig. S-3), showed that they did not interfere with the ratiometric sensing of zinc by **1**, except in the case of  $\text{Co}^{2+}$ ,  $\text{Ni}^{2+}$ ,  $\text{Fe}^{2+}$ , and  $\text{Cu}^{2+}$  the enhancement was less when compared to others. The detection

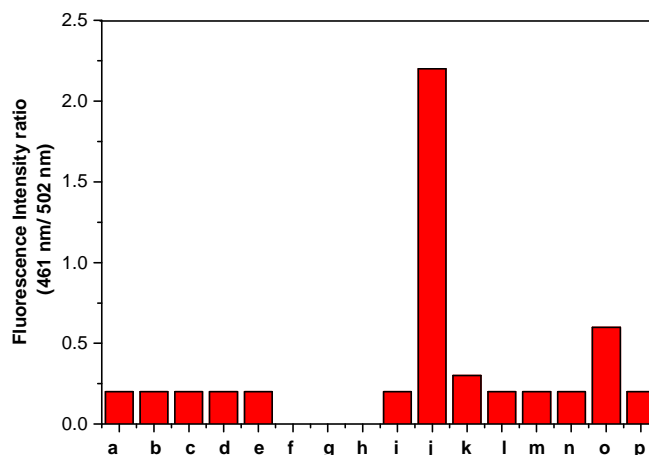


**Figure 7.** Enhancement of fluorescence intensity of **1** (20  $\mu\text{M}$ ) in EtOH/ $\text{H}_2\text{O}$  (9:1) containing HEPES buffer (10 mM, pH 7.4) by addition of 10 equiv of respective metal cation. (a) **1** only, (b) **1** +  $\text{Ag}^+$ , (c) **1** +  $\text{Hg}^{2+}$ , (d) **1** +  $\text{Pb}^{2+}$ , (e) **1** +  $\text{Ca}^{2+}$ , (f) **1** +  $\text{Cu}^{2+}$ , (g) **1** +  $\text{Ni}^{2+}$ , (h) **1** +  $\text{Co}^{2+}$ , (i) **1** +  $\text{K}^+$ , (j) **1** +  $\text{Zn}^{2+}$ , (k) **1** +  $\text{Fe}^{2+}$ , (l) **1** +  $\text{Na}^+$ , (m) **1** +  $\text{Cs}^+$ , (n) **1** +  $\text{Rb}^+$ , (o) **1** +  $\text{Cd}^{2+}$ , (p) **1** +  $\text{Mg}^{2+}$ .

limit of **1** for zinc ion was found to be 10  $\mu\text{M}$  (Fig. S-5) which was found to be sufficient for sensing the zinc ion in the biological system such as brain tissue (0.1–0.5 mM).<sup>25</sup>

**Table 1**  
pK<sub>a</sub> value and wavelength of the absorption and emission maxima of sensors **1** and **2** in EtOH/ $\text{H}_2\text{O}$  (9:1)

Sensor	Absorption max. nm (log $\epsilon$ )		$\Delta\lambda$ (nm)	Emission max. (nm)		$\Delta\lambda$ (nm)	pK <sub>a</sub> <sup>b</sup>
	Free ligand	Complex with $\text{Zn}^{2+}$		Free ligand	Complex with $\text{Zn}^{2+}$		
<b>1</b>	329 (3.74)	384 (3.79)	55	502	461	41	12.02
<b>2</b>	333 (3.91)	333 (3.91)	0	499	499	0	11.55
<b>1</b> <sup>a</sup>	331 (3.74)	390 (3.74)	59	481	461	20	

<sup>a</sup> In dry  $\text{CH}_3\text{CN}$ .

<sup>b</sup> Calculated with 20  $\mu\text{M}$  of **1** and **2** in EtOH/ $\text{H}_2\text{O}$  (9:1) containing 0.1 M KCl within a pH range 8–13 (Fig. S-4).<sup>14b</sup>

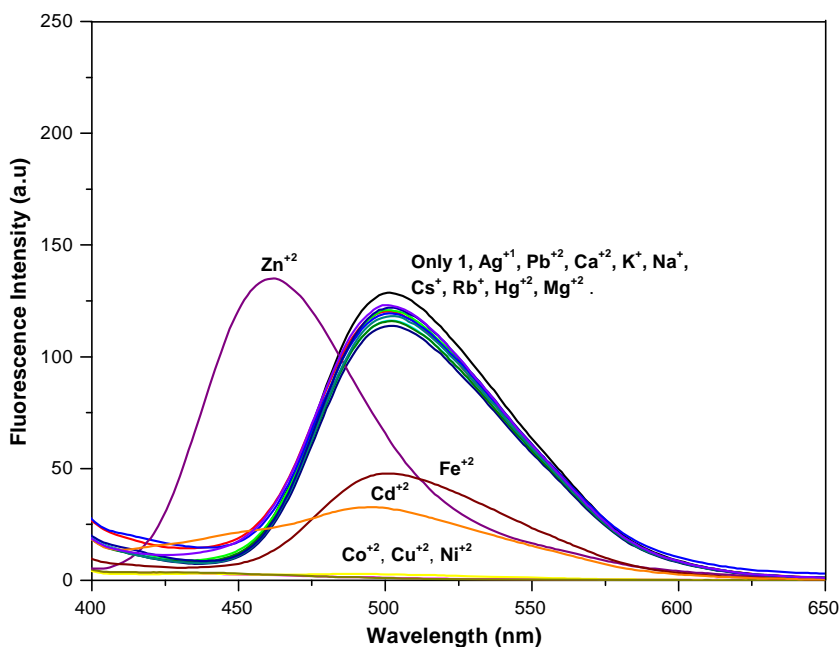


**Figure 6.** Fluorescence spectra of **1** (20  $\mu\text{M}$ ) in EtOH/ $\text{H}_2\text{O}$  (9:1) containing HEPES buffer (10 mM, pH 7.4) upon addition of various metal cations (each concentration was 200  $\mu\text{M}$ ) with an excitation wavelength of 345 nm.

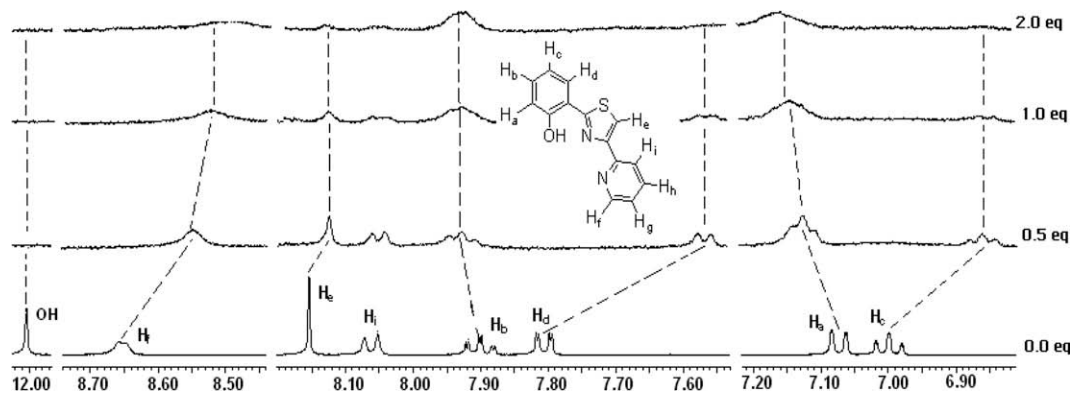


Figure 8. Partial  $^1\text{H}$  NMR spectra of **1** with  $\text{Zn}(\text{ClO}_4)_2$  in  $\text{CD}_3\text{CN}$ .

To get further insight regarding the nature of the zinc complexation, cation recognition was evaluated using  $^1\text{H}$  NMR in  $\text{CD}_3\text{CN}$ . A partial  $^1\text{H}$  NMR spectrum of **1**, upon addition of zinc cation, is shown in Figure 8. Notably, when 1 equiv of zinc cation was added, the signals of  $\text{H}_a$  and  $\text{H}_b$  shifted downfield due to the deshielding effect of the metal ion. But in the case of protons  $\text{H}_c$ ,  $\text{H}_d$ ,  $\text{H}_e$ , and  $\text{H}_f$  experienced a clear upfield shift. It possibly resulted from phenol–metal  $\pi$ – $d$  orbital interaction through space.<sup>26</sup> The  $-\text{OH}$  proton peak disappears due to deprotonation.

In summary a new ratiometric chemosensor **1** has been developed for zinc ion utilizing strong coordination of zinc cation on the phenolic oxygen and thiazole and pyridine nitrogen atoms, and thus disruption of ESIPT mechanism. Upon complexation with zinc ion, this sensor exhibits a blue shift (41 nm) in the emission spectrum. The strong binding affinity with zinc ion is successfully achieved by incorporating a pyridine group as the binding ligand into the fluorophore.

### Acknowledgment

This work was supported by the Kyungpook National University Research Fund, 2009.

### Supplementary data

Supplementary data associated with this article can be found in the online version, at doi:10.1016/j.tetlet.2009.07.078.

### References and notes

- Valeur, B. *Molecular Fluorescence Principles and Applications*; Wiley-VCH Verlag GmbH: New York, 2001.
- de Silva, J. J. R. F.; Williams, R. J. P. *Zinc: Lewis Acid Catalysis and Regulation. In The Biological Chemistry of Elements: The Inorganic Chemistry of Life*, 2nd ed.; Oxford UP: New York, 2001.
- Beyersmann, D.; Haase, H. *Biometals* **2001**, *14*, 331.
- (a) Cuajungco, M. P.; Lees, G. J. *Brain Res.* **1997**, *23*, 219; (b) Takeda, A. *Biometals* **2001**, *14*, 343.
- (a) Frederickson, C. J.; Kasarskis, E. J.; Ringo, D.; Frederickson, R. E. *J. Neurosci. Methods* **1987**, *20*, 91; (b) Zalewski, P. D.; Forbes, I. J.; Betts, W. H. *Biochem. J.* **1993**, *296*, 403; (c) Mikata, Y.; Yamanaka, A.; Yamashita, A.; Yano, S. *Inorg. Chem.* **2008**, *47*, 7295.
- (a) Burdette, S. C.; Walkup, G. K.; Spingler, B.; Tsien, R. Y.; Lippard, S. J. *J. Am. Chem. Soc.* **2001**, *123*, 7831; (b) Hirano, T.; Kikuchi, K.; Urano, Y.; Nagano, T. *J. Am. Chem. Soc.* **2002**, *124*, 6555; (c) Gee, K. R.; Zhou, Z. L.; Qian, W. J.; Kennedy, R. J. *Am. Chem. Soc.* **2002**, *124*, 776.
- (a) Lim, N. C.; Bruckner, C. *Chem. Commun.* **2004**, 1094; (b) Komatsu, K.; Urano, Y.; Kojima, H.; Nagano, T. *J. Am. Chem. Soc.* **2007**, *129*, 13447.
- (a) Koike, T.; Watanabe, T.; Aoki, S.; Kimura, E.; Shiro, M. *J. Am. Chem. Soc.* **1996**, *118*, 12696; (b) Hanaoka, K.; Kikuchi, K.; Kojima, H.; Urano, Y.; Nagano, T. *J. Am. Chem. Soc.* **2004**, *126*, 12470.
- Taki, M.; Watanabe, Y.; Yukio, Y. *Tetrahedron Lett.* **2009**, *50*, 1345.
- (a) Van Dongen, E.; Dekkers, L. M.; Spijker, K.; Meijer, E. W.; Klomp, L. W. J.; Merckx, M. *J. Am. Chem. Soc.* **2006**, *128*, 10754; (b) Bozym, R. A.; Thompson, R. B.; Stoddard, A. K.; Fierke, C. A. *ACS Chem. Biol.* **2006**, *1*, 103; (c) Evers, T. H.; Appelhof, M. A. M.; de Graaf-Heuvelmans, P.; Meijer, E. W.; Merckx, M. *J. Mol. Biol.* **2007**, *374*, 411; (d) Evers, T. H.; Appelhof, M. A. M.; Meijer, E. W.; Merckx, M. *Protein Eng. Des. Sel.* **2008**, *21*, 529.
- (a) Komatsu, K.; Kikuchi, K.; Kojima, H.; Urano, Y.; Nagano, T. *J. Am. Chem. Soc.* **2005**, *127*, 10197; (b) Burdette, S. C.; Frederickson, C. J.; Bu, W.; Lippard, S. J. *J. Am. Chem. Soc.* **2003**, *125*, 1778.
- Grynkiewicz, G.; Poenie, M.; Tsien, R. Y. *J. Biol. Chem.* **1985**, *260*, 3440.
- Henary, M. M.; Fahrni, C. J. *J. Phys. Chem. A* **2002**, *106*, 5210.
- (a) Taki, M.; Wolford, J. L.; O'Halloran, T. V. *J. Am. Chem. Soc.* **2004**, *126*, 712; (b) Henary, M. M.; Wu, Y. G.; Fahrni, C. J. *Chem. Eur. J.* **2004**, *10*, 3015.
- (a) Kim, H.-S.; Koh, Y. K.; Choi, J. H. *J. Heterocycl. Chem.* **1998**, *35*, 177; (b) Kim, H.-S.; Park, H. J.; Oh, H. J.; Koh, Y. K.; Choi, J. H.; Lee, D. H.; Cha, G. S.; Nam, H. *Anal. Chem.* **2000**, *72*, 4683; (c) Kariuki, B. M.; Lee, S.-O.; Harris, K. D. M.; Kim, H.-S.; Do, K.-S.; Kim, K.-I. *Cryst. Growth Des.* **2002**, *2*, 309; (d) Kim, H.-S.; Do, K. S.; Kim, K. S.; Shim, J. H.; Cha, G. S.; Nam, H. *Bull. Korean Chem. Soc.* **2004**, *25*, 1465.
- Hiraoka, S.; Yi, T.; Shiro, M.; Shinoya, M. *J. Am. Chem. Soc.* **2002**, *124*, 14510.
- Kim, H.-S.; Kim, D.-H.; Kim, K. S.; Choi, J.-H.; Choi, H. J.; Kim, S. H.; Shim, J. H.; Cha, G. S.; Nam, H. *Talanta* **2007**, *71*, 1986.
- Kim, B. H.; Hong, H. P.; Cho, K. T.; On, J. H.; Jun, Y. M.; Jeong, I. S.; Cha, G. S.; Nam, H. *Talanta* **2005**, *66*, 794.
- Shim, J. H.; Jeong, I. S.; Lee, M. H.; Hong, H. P.; On, J. H.; Kim, K. S.; Kim, H.-S.; Kim, B. H.; Cha, G. S.; Nam, H. *Talanta* **2004**, *63*, 61.
- Keck, J.; Kramer, H. E. A.; Port, H.; Hirsch, T.; Fischer, P.; Rytz, G. *J. Phys. Chem.* **1996**, *100*, 14468.
- Das, K.; Sarkar, N.; Majumdar, D.; Bhattacharyya, K. *Chem. Phys. Lett.* **1992**, *198*, 443.
- Mosquera, M.; Penedo, J. C.; Rios Rodriguez, M. C.; Rodriguez-Prieto, F. J. *Phys. Chem.* **1996**, *100*, 5398.
- Santra, S.; Krishnamoorthy, G.; Dogra, S. K. *J. Phys. Chem. A* **2000**, *104*, 476.
- Li, H.; Gao, S.; Xi, Z. *Inorg. Chem. Commun.* **2009**, *12*, 300.
- Bush, A. I. *Curr. Opin. Chem. Biol.* **2000**, *4*, 184.
- Lu, C.; Xu, Z.; Cui, J.; Zhang, R.; Qian, X. *J. Org. Chem.* **2007**, *72*, 3554.